journal of the mechanical behavior of biomedical materials 110 (2020) 103866

Contents lists available at ScienceDirect

Journal of the Mechanical Behavior of Biomedical Materials

journal homepage: http://www.elsevier.com/locate/jmbbm

Empirical relationships between bone density and ultimate strength: A literature review

Ingmar Fleps [a,*,1], Hassan Bahaloo [b,1], Philippe K. Zysset [c], Stephen J. Ferguson [a], Halldór Pálsson [b], Benedikt Helgason [a]

[a] Institute for Biomechanics, ETH-Zürich, Zürich, Switzerland
[b] Faculty of Industrial Engineering, Mechanical Engineering and Computer Science, School of Engineering and Natural Sciences, University of Iceland, Reykjavik, Iceland
[c] ARTORG Center for Biomedical Engineering Research, University of Bern, Bern, Switzerland

ARTICLE INFO

Keywords:
Finite element
Computed tomography
Bone
Strength
Density

ABSTRACT

Introduction: Ultimate strength-density relationships for bone have been reported with widely varying results. Reliable bone strength predictions are crucial for many applications that aim to assess bone failure. Bone density and bone morphology have been proposed to explain most of the variance in measured bone strength. If this holds true, it could lead to the derivation of a single ultimate strength-density-morphology relationship for all anatomical sites.

Methods: All relevant literature was reviewed. Ultimate strength-density relationships derived from mechanical testing of human bone tissue were included. The reported relationships were translated to ultimate strength-apparent density relationships and normalized with respect to strain rate. Results were grouped based on bone tissue type (cancellous or cortical), anatomical site, and loading mode (tension vs. compression). When possible, the relationships were compared to existing ultimate strength-density-morphology relationships.

Results: Relationships that considered bone density and morphology covered the full spectrum of eight-fold inter-study difference in reported compressive ultimate strength-density relationships for trabecular bone. This was true for studies that tested specimens in different loading direction and tissue from different anatomical sites. Sparse data was found for ultimate strength-density relationships in tension and for cortical bone properties transverse to the main loading axis of the bone.

Conclusions: Ultimate strength-density-morphology relationships could explain measured strength across anatomical sites and loading directions. We recommend testing of bone specimens in other directions than along the main trabecular alignment and to include bone morphology in studies that investigate bone material properties. The lack of tensile strength data did not allow for drawing conclusions on ultimate strength-density-morphology relationships. Further studies are needed. Ideally, these studies would investigate both tensile and compressive strength-density relationships, including morphology, to close this gap and lead to more accurate evaluation of bone failure.

1. Introduction

Bone is a heterogeneous, anisotropic tissue that plays an important biomechanical role in the human body. Studying the mechanical properties of bone is of major importance for applications such as osteoporosis and injury prevention. Quantitative X-ray Computed Tomography (CT) based finite element models (FEMs) of bones on the organ scale that are frequently used in biomechanical research, are slowly finding their way into clinical practice (Pisu et al., 2019; Sternheim et al., 2018). The workflow for constructing these models conceptually consists of extracting the bone geometry of interest from the CT image data, also known as segmentation; generating an FE mesh; and subsequently applying heterogeneous CT grey level based material properties to the finite elements (Pahr and Zysset, 2009; Poelert et al., 2013; Viceconti et al., 2004). The empirical relationships between the CT grey level values and the mechanical properties of the bone tissue are of particular

* Corresponding author. Institute for Biomechanics, ETH Zürich, Hönggerbergring 64, HPP-O23 CH, 8093, Zürich, Switzerland.
E-mail address: ingmar.fleps@hest.ethz.ch (I. Fleps).
[1] These authors contributed equally to this work.

https://doi.org/10.1016/j.jmbbm.2020.103866
Received 17 March 2020; Received in revised form 6 May 2020; Accepted 17 May 2020
Available online 3 June 2020

interest with respect to the accuracy of the FEMs (Eberle et al., 2013; Helgason et al., 2016; Nishiyama et al., 2013). These relationships are commonly derived from direct mechanical testing of bone cores of various shapes and sizes (Linde and Hvid, 1989), for which density or bone volume fraction is measured, retrieved from different species and anatomical sites (Carter and Hayes, 1977). Dozens of such relationships, between densitometric measures and modulus of elasticity (*modulus-density relationships*) (Helgason et al., 2008), densitometric measures and yield strength (*yield strength-density relationships*) (Morgan and Keaveny, 2001) or densitometric measures and ultimate strength (*ultimate strength-density relationships*) (Linde et al., 1992), have been published in the literature.

A framework for inter-study comparison of modulus-density relationships was introduced by Helgason et al. (2008) that concluded that more than ten-fold inter-study difference in modulus was present at any apparent density range. This was in agreement with the findings of Linde et al. (1992). The difference could not be explained solely by methodological discrepancies, such as different sample geometries, boundary conditions during mechanical testing or different anatomical sites. Assessing the effect of trabecular architecture (or bone morphology) on the mechanical response of bone specimens was not a part of the review by Helgason et al. since at the time studies did generally not quantify bone morphology. However, ultrasound measurements and computational homogenisation of trabecular bone cubic volume elements support the observation that trabecular orientation or fabric (Cowin, 1985) contributes significantly to the determination of anisotropic elastic properties (Turner et al., 1990; Zysset et al., 1998; Kabel et al., 1999; Zysset, 2003). In fact, assuming homogeneous tissue properties in a computer model, up to 97% of the variation in elastic properties of human trabecular bone can be explained by volume fraction and fabric, and no further morphological parameter improves that performance (Maquer et al., 2015). The inclusion of heterogeneous tissue properties did not have a strong effect on these elastic properties (Gross et al., 2012). Morgan et al. (2003) suggested that empirical density-modulus relationships depend on anatomical sites, but this dependence seems to disappear when fabric is accounted for (Matsuura et al., 2008; Gross et al., 2013). Furthermore, these observations could indicate that the large inter-study difference in modulus at any given density range reported by Linde et al. (1992) and Helgason et al. (2008) could at least partially be explained by differences in bone morphology.

Yield strength-density and yield-strength-morphology relationships have been investigated both experimentally and computationally for human trabecular bone. In general, yield strength correlates highly with modulus and exhibits similar dependences with density and morphology (Morgan and Keaveny, 2001; Rincón-Kohli and Zysset, 2009). Experimentally, volume fraction and fabric explain from 71 to 93% of the variation in yield strength (Matsuura et al., 2008; Rincón-Kohli and Zysset, 2009), while computationally, they explain up to 98% of the variation in yield properties (Musy et al., 2017). Again, no other morphological variable helps improve the latter result and observed differences between anatomical sites may well be explained by fabric. Testing numerous human bone specimens retrieved from multiple anatomical sites, across a broad range of bone morphology, Matsuura et al. (2008) and Charlebois et al. (2010) found significantly better correlation between their experimental results and their regression models for both modulus of elasticity and ultimate strength when normalizing their data with respect to trabecular architecture. In other words, there is evidence in the literature to suggest that inter-study differences reported for modulus-density relationships, yield strength-density relationships, and ultimate strength-density relationships can to a large extent be explained by inter-study differences in bone morphology. Despite of this, the use of density-morphology based relationships to describe mechanical properties of bone have seen limited use in FEM studies. This can be explained by the fact that deriving morphological information from clinical CT scans is challenging due to insufficient image resolution. This, however, does not diminish the importance of understanding how morphology, or lack of the inclusion of morphology based material properties in FEM studies, affects the accuracy of FEM-based assessment of whole bone strength.

A systematic review of ultimate strength-density relationships reported in the literature has not yet been published despite the fact that for many applications, the ultimate mechanical resistance of bone is of major importance. Intuitively, one could expect the spread in ultimate strength-density relationships reported in the literature to be smaller than the spread in modulus-density relationships and yield strength-density relationships. This is because modulus-density relationships and yield strength-density relationships rely on accurate displacement measurements during mechanical testing, which is known to be challenging to achieve. However, ultimate strength-density relationships are independent of displacement measurements. It is thus reasonable to hypothesize that the spread in ultimate strength-density relationships reported in the literature can to a large extent be explained by variation in bone morphology, at least in the cancellous bone range where bone morphology is more variable than it is in cortical bone.

Another aspect related to yield or ultimate bone strength, which is of considerable interest for assessing load bearing capacity of whole bone, pertains to tension-compression asymmetry. It is well accepted in the literature, that modulus of elasticity in tension and compression on the apparent level are similar (Keaveny et al., 1994) and evidence exists to suggest that there is a tension-compression asymmetry in both yield strength (Keaveny et al., 1994) and ultimate strength (Burstein et al., 1976). However, to which extent tension-compression asymmetry applies over the full apparent density range for yield or ultimate strength is unclear.

In the present study, we reviewed the relevant literature reporting experimental ultimate bone strength–density relationships, followed by a systematic inter-study comparison of these relationships using the framework published by Helgason et al. (2008). The aim of this review was two fold: First, to investigate whether the literature supports the hypothesis that inter-study variance in reported ultimate strength-density relationships can be explained by differences in bone morphology; Second, to assess tension-compression asymmetry in ultimate strength density-relationships reported in the literature.

2. Materials and methods

2.1. Literature search

We carried out a systematic literature search on PubMed using the search term "(((((((((bone) OR femur) OR vertebra) OR tibia))) AND ((((tensile strength) OR compressive strength) OR "Stress, Mechanical"))) AND ((((density) OR content) OR volume))) AND Humans [Mesh])". This search resulted in 2667 articles. Using our study inclusion and exclusion criteria, a review of the manuscript titles reduced the number of articles down to 237. Further review of the article abstracts reduced the number of relevant articles down to 123. These articles were evaluated based on their full manuscript to identify studies that passed the inclusion and exclusion criteria. Additional studies cited within these articles were added if they met the inclusion criteria. A total of 30 studies were included in this review for inter-study comparison.

2.2. Study inclusion and exclusion criteria

The most commonly applied experimental technique for measuring mechanical properties of bone tissue as a function of densitometric variables, is direct mechanical testing of bone cores using materials testing machines. The term "ultimate strength" of bone cores (σ_u) is generally reserved for the maximum force recorded by a load cell during these tests divided by the nominal cross-sectional area of the specimens in the failure zone. Only studies that used this definition of ultimate strength were included in the review. Studies that measured ultimate strength, using the method described above, were included for further

analysis, independent of the terminology used by the study authors. This applied e.g. for studies that used the term “yielding strength” or “ultimate yield stress” to describe ultimate force divided by specimen cross-sectional area (Sun et al., 2008; Britton and Davie, 1990).

2.3. Other inclusion and exclusion criteria were as follows

- To limit the effect of the measurement method, only studies where ultimate strength was measured by direct mechanical testing in tension or compression were included. Studies based on ultrasound or indentation methods were excluded.
- Only studies that reported empirical relationships based on the following densitometric measures were included: bone volume fraction (*BVF*), equivalent quantitative computed tomography mineral density (ρ_{QCT}), apparent ash density (ρ_{ash}), apparent dry density (ρ_{dry}) and apparent wet density (ρ_{app}). The exact definition of these densitometric measures varies from study-to-study. To minimize the inter-study difference we use the definition of densitometric measures found in Helgason et al. (2008) when determining which metric study authors are reporting independent of the terminology the authors of the original study use. These definitions of densitometric measures from Helgason et al. (2008) are listed in Table 1, for clarity and context.
- Studies testing only animal bones were excluded from this review because some species are known to have bones with different mechanical properties to that of human bones (Currey, 2004). However, studies reporting results from testing a mixture of human and animal bone specimens were included.
- Studies in which specimens were not tested fresh frozen or fresh and in wet conditions were excluded since drying and other specimen preservation procedures have been reported to significantly alter tissue mechanical properties (Martin and Sharkey, 2001).
- Studies on bone samples from donors that at the time of death had diseases which could compromise bone strength were excluded unless authors would pool such data with data from donors with healthy bone tissue.
- Studies that reported ultimate strength-density-morphology relationships were included in the review. For these studies, ultimate strength was noted as $\sigma_{u,i}$ when authors reported ultimate strength as a function of either MIL_i or m_i where "i" refers to a principal direction of the fabric tensor. When authors report ultimate strength as a function of the fabric value along the test axis, the ultimate strength was noted as $\sigma_{u,test}$.

Furthermore, studies that reported ultimate strength-density relationships based on 3-point or 4-point bending tests were excluded from this review. We support this decision based on the uncertainty associated with quantifying ultimate material strength from the force data measured during beam testing. This applies in particular for materials, such as bone, that may undergo significant non-linear deformation when loaded to failure and to which extent may depend on e.g. tension-compression asymmetry in the material strength. Researchers have tried to address this by introducing correction factors when deriving ultimate strength-density relationships based on bending tests. However, consensus on the value of the correction factors (Keller et al., 1990; Lotz et al., 1991) or whether to use them at all (Snyder and Schneider, 1991) does not exist in the literature.

2.4. Selection criteria for strength–density relationships

Many of the studies that were reviewed report multiple ultimate strength-density relationships. In these cases, selection criteria for what to include and what to exclude in the review was defined as follows:

- From studies, that report different ultimate strength–density relationships depending on anatomical site, all relationships were included. From studies that report multiple ultimate strength-density relationships for multiple test directions, all relationships were included. When multiple empirical relationships were derived from the same data in the same study, only the relationship with the highest coefficient of determination was included.
- Ultimate strength-density relationships, for which densitometric and strength information were not derived from the same set of specimens, were excluded (see e.g. Tanaka et al., 2001).
- From studies that derived ultimate strength-density relationships for both minimum specimen *BVF* and average specimen *BVF*,only the relationships based on the latter were included (Perilli et al., 2007, 2008; Tassani et al., 2010). This is to allow for an easier comparison to other studies in the literature, that generally report the results from regression between ultimate strength and average densitometric measures across the full or a large part of the specimen volume.
- When studies report results in the form of ρ_{QCT}, only studies that calibrate the ρ_{QCT} data using hydroxyapatite phantoms or dipotassium hydrogen phosphate (K_2HPO_4) phantoms were included.
- When studies report separate ultimate strength-density relationships for male and female donors respectively (see e.g. McCalden and McGeough, 1997), only relationships from the pooled data were included if they were reported in the original study.
- If a strain rate was specified for preconditioning cycles within the linear elastic range prior to testing to failure, but without strain rate explicitly being specified for testing to failure, the strain rate during preconditioning was assumed to apply for testing to failure (see e.g. Linde and Hvid, 1989).
- When studies report results from testing specimens with different specimen geometry (see e.g. Linde et al., 1992), only the ultimate strength-density relationship with the highest coefficient of determination was included in the review.

Table 1
Definitions of bone densities and bone morphological variables. *Hydrated tissue mass or wet tissue mass:* The specimen mass weighted in air after defatting, rehydration, centrifuging and drying on a blotting paper (Galante et al., 1970). *Dry tissue mass:* The specimen mass weighted in air after defatting and drying at moderate temperatures for more than 4 h. *Ash mass:* The specimens weight after defatting and heating in a furnace at temperature of 500 °C or more for approximately 24 h (Galante et al., 1970). *Bone tissue volume:* Volume of bone excluding pores measured either by Archimedes principle (see e.g. Galante et al., 1970) or by X-ray Computed Tomography (see e.g. Rincón-Kohli and Zysset, 2009).

Density	
$\rho_{real}\left[\frac{g}{cm^3}\right] = Real\ (tissue)\ density = \frac{hydrated\ tissue\ mass}{bone\ tissue\ volume}$	Galante et al. (1970)
$\rho_{app}\left[\frac{g}{cm^3}\right] = Apparent\ density = \frac{hydrated\ tissue\ mass}{total\ specimen\ volume}$	Galante et al. (1970)
$\rho_{wet}\left[\frac{g}{cm^3}\right] = Apparent\ wet\ density = \frac{hydrated\ tissue\ mass}{total\ specimen\ volume}$	Keyak et al. (1994)
$\rho_{dry}\left[\frac{g}{cm^3}\right] = Apparent\ dry\ density = \frac{dry\ tissue\ mass}{total\ specimen\ volume}$	Keller (1994), Keyak et al. (1994)
$\rho_{ash}\left[\frac{g}{cm^3}\right] = Apparent\ ash\ density = \frac{ash\ mass}{total\ specimen\ volume}$	Galante et al. (1970)
$\rho_{QCT}\left[\frac{g}{cm^3}\right] = QCT\ equivalent\ mineral\ density$	Keyak et al. (1994)
$BVF = Bone\ volume\ fraction = \frac{bone\ tissue\ volume}{total\ specimen\ volume}$	Gibson (1985)
$MIL_n = \frac{1}{\sqrt{n.An}} = mean\ intercept\ length\ along\ direction\ n$	Harrigan and Mann (1984)
$M = \frac{3}{Tr\left(A^{-\frac{1}{2}}\right)}A^{-\frac{1}{2}} = normalised\ fabric\ tensor$	Zysset et al. (1998)
$m_i = normalized\ fabric\ eigenvalue\ along\ eigenvector\ i\ of\ M$	Zysset et al. (1998)
$m_{test} = n.Mn = normalized\ fabric\ along\ testing\ direction\ n$	Zysset et al. (1998)
$DA = degree\ of\ anisotropy = \frac{MIL_{max}}{MIL_{min}} = \frac{Max(m_i)}{Min(m_i)}$	Goulet et al. (1994)

Table 2
Compressive ultimate strength-density relationships from the studies included in the review.

	Study	Site	Type of bone	Densitometric measure	Density range	$\sigma_u(\rho,\dot{\varepsilon})$ [MPa]	$\sigma_u\left(\rho_{app}\left[\frac{g}{cm^3}\right]\right)$ [MPa], at $\dot{\varepsilon} = 0.01\left[\frac{1}{s}\right]$	Test condition	Specimen geometry cuboid (B x W x H) cylinder (D x H) [mm]	Strain rate $\left[\frac{1}{s}\right]$	N	R^2
1	Galante et al. (1970)	Vertebra Vertebra Vertebra	Trabecular	$\rho_{app}\left[\frac{g}{cm^3}\right]$ AP $\rho_{app}\left[\frac{g}{cm^3}\right]$ SI $\rho_{app}\left[\frac{g}{cm^3}\right]$ ML	0.147-0.357 0.159-0.271 0.170-0.300	$\sigma_u\left[\frac{kp}{cm^2}\right] = -7.61 + 71.74 \cdot \rho_{app}$ $\sigma_u\left[\frac{kp}{cm^2}\right] = -3.79 + 116.93 \cdot \rho_{app}$ $\sigma_u\left[\frac{kp}{cm^2}\right] = -5.04 + 55.14 \cdot \rho_{app}$	$\sigma_u = -0.72 + 6.82 \cdot \rho_{app}$ $\sigma_u = -0.36 + 11.12 \cdot \rho_{app}$ $\sigma_u = -0.48 + 5.25 \cdot \rho_{app}$	NR	10 x 10	0.0167	17 14 15	NR
2	Carter and Hayes (1977)	Pooled	Trabecular	$\rho_{app}\left[\frac{g}{cm^3}\right]$	0.07 - 1.8[a] RFG	$\sigma_u = 68 \cdot \dot{\varepsilon}^{0.06} \rho_{app}{}^{2}$	$\sigma_u = 51.58 \cdot \rho_{app}{}^{2}$	Confined compression	20.6 x 5	0.001–10	124	NR
3	Klever et al. (1985)	Tibia	Trabecular	$\rho_{app}\left[\frac{g}{cm^3}\right]$	0.22 – 0.58	$\sigma_u = 38 \cdot \rho_{app}{}^{1.5}$	$\sigma_u = 38 \cdot \rho_{app}{}^{1.5}$	Platen	8 x 8 x 8	0.01	17	0.77
4	Hansson et al. (1987)	Vertebra	Trabecular	$\rho_{dry}\left[\frac{g}{cm^3}\right]$	0.05 – 0.3 RFG	$\sigma_u = 85.3 \cdot \rho_{dry}{}^{2.24}$	$\sigma_u = 71.21 \cdot \rho_{app}{}^{2.24}$	Platen	10 x 10 x 10	0.009	231	0.76
5	Mosekilde et al. (1987)	Vertebra	Trabecular	$\rho_{ash}\left[\frac{g}{cm^3}\right]$	0.07 – 0.24 RFG	$\sigma_u = 78.2 \cdot \rho_{ash}{}^{1.8}$	$\sigma_u = 27.31 \cdot \rho_{app}{}^{1.8}$	Platen	7 x 5	0.0067	40	0.83
6	Lang et al. (1988)	Vertebra	Trabecular	$\rho_{QCT}\left[\frac{mg}{cm^3}\right]^{1}$	45 – 200 RFG	$\sigma_u = 3.84 \cdot 10^{-5} \cdot \rho_{QCT}{}^{2.12}$	$\sigma_u = 101.0 \cdot (0.52 \cdot \rho_{app} - 0.04)^{2.12}$	NR	4 x 13	0.001	76	0.5
7	Hvid et al. (1989)	Tibia	Trabecular	$\rho_{ash}\left[\frac{g}{cm^3}\right]$	0.05 – 0.34 RFG	$\sigma_u = 70.38 \cdot \rho_{ash}{}^{1.596}$	$\sigma_u = 27.07 \cdot \rho_{app}{}^{1.60}$	Platen	7.5 x 7.5	0.01	94	0.81
8	Linde and Hvid (1989)	Tibia	Trabecular	$\rho_{dry}\left[\frac{g}{cm^3}\right]$	0.237 (SD 0.055)	$\sigma_u = 69 \cdot \rho_{dry}{}^{2.1}$	$\sigma_u = 57.92 \cdot \rho_{app}{}^{2.1}$	Platen, oiled	7.5 x 7.5	0.01	33	0.88
9	Odgaard et al. (1989)	Tibia	Trabecular	$\rho_{dry}\left[\frac{g}{cm^3}\right]$	0.2 – 0.8 RFG	$\sigma_u = 17.05 \cdot \rho_{dry}{}^{1.82}$	$\sigma_u = 18.85 \cdot \rho_{app}{}^{1.82}$	Platen, oiled	5 x 7.5	0.00015	50	0.83
10	Britton and Davie (1990)	Ilium Vertebra	Trabecular	$\rho_{app}\left[\frac{mg}{cm^3}\right]$	130 – 870 RFG 90 – 560 RFG	$\sigma_u = -2.18 + 0.0125 \cdot \rho_{app}$ $\sigma_u = -1.53 + 0.016 \cdot \rho_{app}$	$\sigma_u = -2.33 + 13.36 \cdot \rho_{app}$ $\sigma_u = -1.64 + 17.10 \cdot \rho_{app}$	NR	8 x 5	0.0033	154 234	0.80 0.76
11	Lotz et al. (1990)	Femur	Trabecular	$\rho_{app}\left[\frac{g}{cm^3}\right]$	0.18 - 0.95 RFG	$\sigma_u = 25 \cdot \rho_{app}{}^{1.8}$	$\sigma_u = 23.41 \cdot \rho_{app}{}^{1.8}$	Platen	9 x 5	0.03	49	0.93
12	Linde et al. (1991)	Tibia	Trabecular	$\rho_{dry}\left[\frac{g}{cm^3}\right]$	0.22 - 0.59 RFG	$\sigma_u = 40.2 \cdot \dot{\varepsilon}^{0.073} \rho_{dry}{}^{1.65}$	$\sigma_u = 25.03 \cdot \rho_{app}{}^{1.65}$	Platen, oiled	5.5 x 8.25	0.0001–10	60	0.86
13	Anderson M JSkinner (1992)	Tibia	Trabecular	$\rho_{dry}\left[\frac{g}{cm^3}\right]$	0.14 - 0.49 RFG	$\sigma_u = 51.3 \cdot \rho_{dry}{}^{2.09}$	$\sigma_u = 43.10 \cdot \rho_{app}{}^{2.09}$	Platen	10 x 10 x 20	0.01	30	NR
14	Linde et al. (1992)	Tibia	Trabecular	$\rho_{dry}\left[\frac{g}{cm^3}\right]$	0.16 – 0.78	$\sigma_u = 76.5 \cdot \rho_{dry}{}^{2.23}$	$\sigma_u = 63.52 \cdot \rho_{app}{}^{2.23}$	Platen, oiled	7.5 x 7.5	0.01	31	0.88
15	Goulet et al. (1994)	Pooled	Trabecular	BVF	0.06 – 0.36	$\log(\sigma_{u,i}) = 2.79 + 1.44 \cdot \log(BVF) + 2.41 \cdot \log(MIL_i) - 0.58 \cdot \log(DA)$	$\sigma_{u,i} = 264.49 \cdot \rho_{app}^{1.44} MIL_i^{2.41} \cdot DA^{-0.58}$	Platen	8 x 8 x 8	0.01	104	0.91
16	Keller (1994)	Vertebra Femur Pooled	Trabecular Cortical Both	$\rho_{ash}\left[\frac{g}{cm^3}\right]$	0.028–0.182 0.092-1.221 0.028-1.221	$\sigma_u = 284 \cdot \rho_{ash}{}^{2.27}$ $\sigma_u = 116 \cdot \rho_{ash}{}^{2.03}$ $\sigma_u = 117 \cdot \rho_{ash}{}^{1.93}$	$\sigma_u = 73.10 \cdot \rho_{app}{}^{2.27}$ $\sigma_u = 34.47 \cdot \rho_{app}{}^{2.03}$ $\sigma_u = 36.91 \cdot \rho_{app}{}^{1.93}$	Platen, oiled	10 x 10 x 10 8 x 8 x 8 combined	0.01	199 297 496	0.79 0.93 0.97
17	Keyak et al. (1994)	Tibia SI Tibia AP Tibia ML	Trabecular	$\rho_{ash}\left[\frac{g}{cm^3}\right]$	0.055 – 0.27 RFG	$\sigma_u = 137 \cdot \rho_{ash}{}^{1.88}$ $\sigma_u = 58.0 \cdot \rho_{ash}{}^{1.64}$ $\sigma_u = 70.2 \cdot \rho_{ash}{}^{2.05}$	$\sigma_u = 44.53 \cdot \rho_{app}{}^{1.88}$ $\sigma_u = 21.76 \cdot \rho_{app}{}^{1.64}$ $\sigma_u = 20.60 \cdot \rho_{app}{}^{2.05}$	Platen	15 x 15 x 15	0.01	12 12 12	0.91 0.93 0.80
18	Ebbesen et al. (1997)	Ilium (Female)	Trabecular	$\rho_{ash}\left[\frac{mg}{cm^3}\right]$	70 – 440 RFG	$\sigma_u = 1.31 \cdot 10^{-5} \cdot \rho_{ash}{}^{2.25}$ $\sigma_u = 2.39 \cdot 10^{-5} \cdot \rho_{ash}{}^{2.15}$	$\sigma_u = 19.66 \cdot \rho_{app}{}^{2.25}$ $\sigma_u = 19.08 \cdot \rho_{app}{}^{2.15}$	NR	7 x 5	0.0067	41 54	0.94 0.94

(*continued on next page*)

Table 2 (*continued*)

	Study	Site	Type of bone	Densitometric measure	Density range	$\sigma_u(\rho,\ \dot{\varepsilon})$ [MPa]	$\sigma_u\left(\rho_{app}\left[\frac{g}{cm^3}\right]\right)$ [MPa], at $\dot{\varepsilon} = 0.01\left[\frac{1}{s}\right]$	Test condition	Specimen geometry cuboid (B x W x H) cylinder (D x H) [mm]	Strain rate $\left[\frac{1}{s}\right]$	N	R^2
		Ilium (Male)										
19	McCalden and McGeough (1997)	Femur	Trabecular	$\rho_{dry}\left[\frac{kg}{m^3}\right]$	220 – 580 RFG	$\log(\sigma_u) = -3.723 + 1.784 \cdot \log(\rho_{dry})$	$\sigma_u = 40.80 \cdot \rho_{app}^{1.79}$	Platen	10 x 10	0.0017	255	0.94
20	Kaneko et al. (2003)	Femur	Cortical	$\rho_{QCT}\left[\frac{mg}{cm^3}\right]$[2]	1176-1271	$\sigma_u = -63.6 + 0.184 \cdot \rho_{QCT}$	$\sigma_u = -69.82 + 100.48 \cdot \rho_{app}$	Clamped	Dumbbell shape 2 x 5 x 6	0.001	8	0.90
21	Kaneko et al. (2004)	Femur	Trabecular	$\rho_{ash}\left[\frac{mg}{cm^3}\right]$	102-331	$\sigma_u = 0.000592 \cdot \rho_{ash}^{1.75}$	$\sigma_u = 36.98 \cdot \rho_{app}^{1.75}$	Platens, extensometer	15 x 15 x 15	0.01	52	0.89
22	Perilli et al. (2007)	Femur	Trabecular	BVF [%]	9 – 44 RFG	$\sigma_u = 0.06 \cdot BVF^{1.67}$	$\sigma_u = 49.19 \cdot \rho_{app}^{1.67}$	End-caps, extensometer	10 x 20	0.01	37	0.84
23	Duchemin et al. (2008)	Femur	Cortical	$\rho_{QCT}\left[\frac{mg}{cm^3}\right]$[3]	422–1457	$\sigma_u = -5.95 + 0.097 \cdot \rho_{QCT}$	$\sigma_u = -16.17 + 66.99 \cdot \rho_{app}$	Platen	3 x 3 x 5	0.002	46	0.72
24	Perilli et al. (2008)	Femur	Trabecular	BVF [%][4]	9 – 44 RFG	$\sigma_u = 0.07 \cdot BVF^{1.65}$	$\sigma_u = 52.96 \cdot \rho_{app}^{1.65}$	End-caps, extensometer	10 x 20	0.01	50	0.84
25	Rincón-Kohli and Zysset (2009)	Pooled	Trabecular	BVF	0.044-0.466[b]	$\sigma_{u,i} = 43.82 \cdot BVF^{1.351} m_i^{2.182}$	$\sigma_{u,i} = 23.34 \cdot \rho_{app}^{1.351} m_i^{2.182}$	End-caps	8.0 x 10	0.00065	17	0.98
26	Tassani et al. (2010)	Femur	Trabecular	BVF [%]	17.5 – 43	$\sigma_u = -6.22 + 0.71 \cdot BVF$	$\sigma_u = -6.22 + 39.45 \cdot \rho_{app}$	End-caps, extensometer	10 x 20	0.01	25	0.53
27	Charlebois et al. (2010)	Pooled	Trabecular	BVF	0.042-0.376	$\sigma_{u,ii} = 48.1 \cdot BVF^{1.75} m_{test}^{3.22}$	$\sigma_u = 19.43 \cdot \rho_{app}^{1.75} m_{test}^{3.22}$	End-caps	7.5 x 11.5	0.0013	148	0.79
28	Cook et al. (2010)	Femur	Trabecular	$\rho_{app}\left[\frac{g}{cm^3}\right]$	0.1-0.4	$\log(\sigma_u) = 1.38 + 1.91 \cdot \log(\rho_{app})$	$\sigma_u = 22.71 \cdot \rho_{app}^{1.91}$	End-caps	9 x NR	0.025	NR	0.63
29	Öhman et al. (2011)	Femur and tibia pooled	Cortical	$\rho_{ash}\left[\frac{g}{cm^3}\right]$	0.59 – 1.29 RFG	$\sigma_u = 144.7 \cdot \rho_{ash}^{2.0}$	$\sigma_u = 38.12 \cdot \rho_{app}^{2}$	End-caps, extensometer	3 x 12 2 x 8	0.1	94	0.91

NR: Not reported. AP: Anterior-posterior direction. SI: Superior-inferior direction. ML: Medial-lateral direction.

[1] ρ_{CT} using a K_2HPO_4 phantom.

[2] ρ_{CT} using a HA phantom.

[3] ρ_{CT}using a HA equivalent phantom.

[4] BVF min was used. This BVF is derived from a sub-volume of the specimen.

[a] Testing range between ρ_{app} of 0.1–0.6 g/cm^3 but ultimate strength-density relationship derived based on the assumption that $\rho_{app} = 1.8$ g/cm.^{3}.

[b] Data provided by authors.

2.5. Inter-study comparison

Inter-study comparison was carried out for two groups; compressive ultimate strength-density relationships and tensile ultimate strength-density relationships, respectively. All ultimate strength-density relationships were normalized to apparent density (ρ_{app}) based on the following mathematical relationships used in the study of Helgason et al. (2008):

$\rho_{app}(\mathrm{g/cm^3}) = \frac{\rho_{ash}}{0.55}$, based on Keyak et al. (1994).

$\rho_{app}(\mathrm{g/cm^3}) = \frac{\rho_{dry}}{0.92}$, based on Keyak et al. (1994).

$\rho_{app}(\mathrm{g/cm^3}) = \frac{BV}{TV} 1.8\ (\mathrm{g/cm^3})$, based on Gibson (1985).

Furthermore, when studies report ultimate strength density-relationships in terms of ρ_{QCT}, where ρ_{QCT} is derived from CT grey levels using hydroxyapatite (HA) phantoms, the following conversion from Schileo et al. (2008) was used to translate ρ_{QCT} (in $\mathrm{g/cm^3}$) to ρ_{ash} (in $\mathrm{g/cm^3}$):

$$\rho_{ash} = 0.0789 + 0.877\rho_{QCT}$$

Corresponding conversion from ρ_{QCT} to ρ_{ash} for studies that derived ρ_{QCT} based on dipotassium hydrogen phosphate phantoms was based on the work of Keyak et al. (1994):

$$\rho_{ash} = 0.0389 + 1.06\rho_{QCT}$$

Since studies test specimens under different strain rates, all strength density relationships were normalized to a strain rate of 0.01/s using this equation from Rice et al. (1988):

$$\sigma_{u,(at\ 0.01/s)} = \left(\frac{0.01/s}{\dot{\varepsilon}_{orig}}\right)^{0.06} \sigma_{u,(at\ orig\ \dot{\varepsilon})}$$

where $\sigma_{u,(at\ orig\ \dot{\varepsilon})}$ is the ultimate strength as reported in the original study, $\dot{\varepsilon}_{orig}$ is the strain rate during the testing in the original study, and $\sigma_{u,(at\ 0.01/s)}$ is the estimated ultimate strength at a strain rate of 0.01/s.

All ultimate strength-density relationships were plotted on the same graph, showing the full apparent density range, as well as for low density range only (0–1 $\mathrm{g/cm^3}$), for readability. When studies reported only the mean and standard deviation (SD) of their densitometric measurements but not range, the corresponding empirical relationship was plotted assuming a symmetric range of ±1.96xSD around the mean of the densitometric variable. For compressive ultimate strength-density-morphology relationships we plotted only a single curve based on the average values of the morphological variables that the authors used in their regression when deriving the empirical relationship (see Table 4 for details).

Separate plots were generated for compressive ultimate strength-density relationships and tensile ultimate strength-density relationships. Additional plots were generated for compressive ultimate strength based on splitting the data up based on anatomical site. This was not done for the tensile strength data due to the low number of studies reporting tensile ultimate strength-density relationships. For studies that reported tensile ultimate strength-density-morphology relationships, we plotted only a single curve based on the average values of the morphological variables that the authors used in their regression when deriving the empirical relationship (see Table 4 for details).

To test our hypothesis that the inter-study difference in ultimate strength-density relationships reported in the literature can be explained by difference in morphology in the cancellous bone range, a separate comparison was carried out by plotting the full range of the ultimate strength-density-morphology relationships on top of the ultimate strength-density relationships. This was done by plotting the upper and lower limits for the ultimate strength-density-morphology relationships overlaid on top of the ultimate strength-density relationships. The upper and lower limits were based on the extreme values of the morphological variables reported by the authors for the respective studies (see Table 4 for details). This comparison was only carried out for the compressive ultimate strength-density relationships and only using the ultimate strength-density-morphology relationships that tested specimen across a broad spectrum of bone morphology.

To assess whether consensus can be found in the literature on the tension-compression asymmetry in ultimate strength as a function of density, a comparison was carried out where the ultimate tensile and ultimate compressive strength-density relationships were plotted on the same graph for the full apparent density range as well as for cancellous bone density range.

3. Results

3.1. All studies

From the 30 studies that passed the review criteria, a total of 41 ultimate strength-density relationships were recorded. Of these relationships, 37 described compressive ultimate strength as a function of density, and 4 described tensile ultimate strength as a function of density. We decided to include the compressive ultimate strength-density relationships from the highly cited study by Carter and Hayes (1977), even though the regression work in the study deviated from the other studies included in this review. The authors based their regression on the assumption that dense cortical bone has a density of 1.8 $\mathrm{g/cm^3}$ and a compressive strength of 221 MPa at a strain rate of 1/s. Goulet et al. (1994) reported different ultimate strength-density-morphology relationships for specimens tested along the anterior-posterior (AP), superior-inferior (SI) and medial-lateral (ML) directions, respectively. From this study, we only included the empirical relationship for the pooled data since all of the relevant morphological data was not available for the different testing directions. Pooling data across different testing directions the Goulet et al. (1994) found an empirical relationship including *BVF*, *MIL* and *DA* to explain the variance in the testing results marginally better than a relationship including only *BVF* and *MIL*. In the inter-study comparison, we used the relationship including *DA* but fixed the value of it to the average reported value (see Table 4 for details).

Table 2 summarizes all the papers that were included in the inter-study comparison for ultimate compressive strength-density and ultimate compressive strength-density-morphology relationships. Table 3 contains the summary of all the ultimate tensile strength-density and the ultimate tensile strength-density-morphology relationships. For each study, the following information and parameters were included in Tables 2 and 3: anatomical site, type of bone, densitometric measure, testing range, testing conditions, specimen dimensions, strain rate, number of samples tested, ultimate strength–density relationship, and the corresponding determination coefficient. A plot of all the compressive ultimate strength relationships as a function of apparent density and normalized with respect to strain rate, is provided in Fig. 1. At any given density in the cancellous bone range (0–1 $\mathrm{g/cm^3}$), the inter-study difference in compressive ultimate strength was almost eight-fold. The tensile ultimate strength relationships are plotted in Fig. 2. Only one of the four tensile relationships found in the literature covered bone in the cancellous bone range. The other three relationships reported results from testing cortical bone. In Fig. 3, the compressive ultimate strength relationships in the cancellous bone range have been split into sub-plots depending on anatomical site.

Influence of morphology

The compressive ultimate strength-density relationships listed in Table 2 are plotted in the cancellous bone density range in Fig. 4, with the full range of the results from ultimate strength-density-morphology studies from Goulet et al. (1994) and Charlebois et al. (2010) overlaid, but these authors tested specimens from multiple anatomical sites across a broad range of bone morphologies (see Table 4 for details). It is evident that the extremes of the pooled results from Goulet et al. (1994) and

Table 3
Tensile ultimate strength-density relationships from the studies included in the review.

	Study	Site	Type of bone	Densitometric measure	Density range	$\sigma_u(\rho, \dot{\varepsilon})$ [MPa]	$\sigma_u\left(\rho_{app}\left[\frac{g}{cm^3}\right]\right)$ [MPa], at $\dot{\varepsilon} = 0.01\left[\frac{1}{s}\right]$	Test condition	Geometry cuboid (B x W x H) cylinder (D x H) [mm]	Strain rate $\left[\frac{1}{s}\right]$	N	R^2
1	McCalden et al. (1993)	Femur	Cortical	[%]	72 – 96	$\sigma_u = -114.22 + 2.389 \cdot BVF$	$\sigma_u = -106.9 + 124.3 \cdot \rho_{app}$	Clamped	Dumbbell shape 2 × 2 × 12	0.03	45	0.76
2	Kaneko et al. (2003)	Femur	Cortical	$\rho_{QCT}\left[\frac{mg}{cm^3}\right]^1$	416–1342	$\sigma_u = -19.8 + 0.0956 \cdot \rho_{QCT}$	$\sigma_u = -24.8 + 52.2 \cdot \rho_{app}$	Clamped	Dumbbell shape 2 x 5 x 6	0.001	41	0.71
3	Duchemin et al. (2008)	Femur	Cortical	$\rho_{QCT}\left[\frac{mg}{cm^3}\right]^2$	402-1448	$\sigma_u = -21.82 + 0.064 \cdot \rho_{QCT}$	$\sigma_u = -32.4 + 47.2 \cdot \rho_{app}$	Clamped	3 x 3 x 15	0.00067	46	0.57
4	Rincón-Kohli and Zysset (2009)	Femur, tibia distal radius vertebra	Trabecular	*BVF*	0.042-0.290[a]	$\sigma_{u,i} = 13.0 \cdot BVF^{0.733} m_{test}^{1.376}$	$\sigma_{u,i} = 9.96 \cdot \rho_{app}^{0.733} m_{test}^{1.376}$	End-caps	8.0 x 10	0.00046	21	0.72

[a] Data provided by authors.

Charlebois et al. (2010) overlap all the compressive ultimate strength-density relationships except the ultimate strength-density-morphology relationship published by Rincón-Kohli and Zysset (2009) that tested specimens from multiple anatomical sites loaded along the strongest trabecular orientation. The specimens were harvested, with the help of radiographs, so that the loading axis would be as close to the strongest specimen axis as possible.

Tension-compression asymmetry

Fig. 5 illustrates a comparison between the tensile and compressive ultimate strength-relationships that passed the inclusion criteria. Two of these studies published both compressive and tensile ultimate strength relationships in the cortical bone range. The tension-compression asymmetry ratio for ultimate strength, at ρ_{app} of 1.8 g/cm^3, was found to be 0.62 and 0.50 according to Kaneko et al. (2003) and Duchemin et al. (2008), respectively. The tension-compression asymmetry ratio for trabecular bone was analysed according to Rincón-Kohli and Zysset (2009) when assuming the anisotropy in both tension and compression corresponding to $m_i = 1.4$, which is close to the average m_i reported by the authors. The asymmetry ratio for ρ_{app} of 0.1 g/cm^3, 0.3 g/cm^3, and 0.5 g/cm^3 were 1.35, 0.68, and 0.5, respectively.

4. Discussion

The first aim of this review was to investigate whether the literature supports the hypothesis that inter-study variance in reported experimental ultimate strength-density relationships for bone can be explained by differences in bone morphology. We found this to hold true for compressive ultimate strength-density relationships in the cancellous bone range; however, drawing similar conclusions for tensile ultimate strength-density relationships is not possible due to lack of data. The second aim of this review was to assess whether a consensus exists in the literature on tension-compression asymmetry in ultimate strength across the full spectrum of bone density. We found insufficient body of literature reporting tensile ultimate-strength relationships in the cancellous bone range to allow for detailed conclusions to be drawn on this aspect of the review.

Despite that inter-study difference in compressive ultimate strength can be as high as eight-fold, at cancellous bone density, we found that the compressive ultimate strength-density-morphology relationships reported by Goulet et al. (1994) and Charlebois et al. (2010) to almost fully explain the inter-study variance across studies in the cancellous bone range (Fig. 4). Whether this holds true after splitting the data depending on anatomical site is unclear because the only site dependent ultimate strength-density-morphology relationships we found in the literature were reported by Matsuura et al. (2008), but this study did not pass our review criteria because specimens were fixed in formalin prior to testing. However, splitting the data depending on anatomic site (Fig. 3) showed that there is difference in *BVF* between sites at least between specimens harvested from vertebra as opposed to other sites, which is by no means a novel finding (see e.g. Matsuura et al., 2008; Rincón-Kohli and Zysset, 2009). Furthermore, Fig. 3 also indicates considerable intra-site spread in the data for all anatomical sites except for specimens harvested from human ilium bone, where only 3 studies are available.

The inter-study difference in ultimate compressive strength for cortical bone density of 1.8 g/cm^3 was found to be around 40%. After excluding the study by Carter and Hayes (1977), which did not measured cortical bone but assumed a literature based strength for an ρ_{app} of 1.8 g/cm^3, the inter-study difference is around 15%. The lower inter-study variance for cortical bone compared to cancellous bone, can at least partially be explained by similarities between studies in terms of how specimens are harvested from long bones and generally loaded along the long bone axis. Furthermore, anisotropy due to trabecular architecture transforms into anisotropy in vascular porosity in dense

Table 4
Range of morphological variables reported in the studies of Goulet et al. (1994), Rincón-Kohli and Zysset (2009), and Charlebois et al. (2010).

Study	Anatomical site	m_{test} average	m_{test} min	m_{test} max	m_i average	m_i min	m_i max	*MIL* average	*MIL* min	*MIL* max	*DA* average
Goulet et al. (1994)	Pooled (C)	–	–	–	–	–	–	0.31	0.19	0.55	1.65
Rincón-Kohli and Zysset (2009)	Pooled (T)[a]	–	–	–	1.395	1.144	1.742	–	–	–	–
Rincón-Kohli and Zysset (2009)	Pooled (C)[a]	–	–	–	1.361	1.171	1.545	–	–	–	–
Charlebois et al. (2010)	Pooled (C)	1.124	0.678	1.510	–	–	–	–	–	–	–

(C): compression; (T): tension; *MIL*: mean intercept length in millimeters; *DA*: degree of anisotropy; m_{test}: normalized fabric tensor value along the testing direction; m_i: normalized fabric tensor value along the eigenvector i closest to the testing direction.
[a] Data provided by the authors.

cortical bone. However, it is a well-known fact that there is tissue level anisotropy in cortical bone. For instance, Reilly and Burstein (1975) reported compressive strength in the transverse directions, for specimens harvested from human femurs, to be 36% lower than compressive strength in the longitudinal direction. The authors reported a corresponding difference for specimens tested in tension to be 61%.

The ultimate strength-density-morphology relationships studied in this review are based on data fitting for specimens tested in the cancellous bone range and apart from that, they do not include tissue level anisotropy. As a result, these relationships cannot be extrapolated to cortical bone density range. If isotropy is assumed ($m_i = 1$), the empirical relationship reported by Charlebois et al. (2010) would predict a compressive strength for cortical bone of 48.1 MPa at a density of 1.8 g/cm^3, which is a lower compressive ultimate strength for dense cortical bone than studies measuring cortical bone are reporting. In other words, although the ultimate strength-density-morphology relationships can explain the inter-study difference in the cancellous bone range, they cannot be extrapolated to predict cortical bone properties. Extending the ultimate strength-density-morphology relationships to cover the full bone density range can be achieved with an adjustment of the exponent in the power fit or with a piecewise power function (see e.g. Dall'Ara et al., 2013).

Limited data is available on ultimate tensile strength-density relationships in the literature. Needless to say, it is not because tensile failure in bone is less important to study than compressive failure. We suspect that this finding could be associated with the fact that testing bone cores in tension is somewhat more challenging than testing them in compression due to different specimen preparation procedures for tensile testes, which optimally would involve milling specimens to dog bone shape and gluing the specimens into end-caps. Only one study reporting ultimate strength-density relationship in the cancellous bone density range passed our inclusion criteria. It should be added though, that the study of Røhl et al. (1991) reported a relationship between tensile ultimate strength and CT attenuation coefficients of the specimens that they tested, but we did not find a way to normalize this densitometric measure in this review. Røhl et al. found ultimate tensile strength to be significantly higher than ultimate compressive strength in specimens harvested from human proximal tibiae. Other studies that compared tensile ultimate strength and compressive ultimate strength of cancellous bone found conflicting evidence. Carter et al., 1980 found no difference between ultimate tensile and ultimate compressive strength. The data reported by Rincón-Kohli and Zysset (2009) showed ultimate tensile strength in the cancellous bone range to be higher than ultimate compressive strength for very low bone mineral densities, but lower than ultimate compressive strength for higher cancellous bone densities. The tension-compression asymmetry ratio for yield stress was reported to be 0.63 and 0.85 by Morgan and Keaveny (2001) and Rincón-Kohli and Zysset (2009), respectively. Since ultimate strength of trabecular bone correlates highly to yield stress, the findings in this review are consistent with the experimental and computational findings for yield strength mentioned in the introduction.

Ultimate tensile strength-density relationships for cortical bone that passed our inclusion criteria, were only found in three studies. All three ultimate strength-density relationships were linear, resulting in unreasonable strength at low density range meaning that they cannot be used for predicting ultimate strength across the full range of apparent bone density. The tension-compression asymmetry ratios for dense cortical bone of 0.62 and 0.50 according to Kaneko et al., 2003 and Duchemin et al., 2008 respectively, are slightly lower than reported by e.g. Burstein et al., 1976 and Reilly and Burstein, 1975 that reported asymmetry ratios of approximately 0.68 and 0.65, respectively.

There are several limitations associated with this review as well as small observations that are worth noting. First, despite our best effort towards normalizing the results of different studies to allow for a meaningful inter-study comparison, several factors not accounted for, may generate inter-study discrepancies. For instance, studies do not generally split up the results depending on donor age despite the fact that ultimate strength of bone tissue is known to decrease with age (Mosekilde et al., 1987; Wang et al., 2002). Specimen preparation, storage, specimen aspect ratio and support end-conditions during mechanical testing can also contribute to inter-study discrepancies. Splitting the data depending on these factors is possible but does not allow for subtle differences to be detected because the trabecular orientation appears to be the largest contributor to the inter-study differences. However, we have no way of normalizing the data from different studies with respect to architecture when bone architecture is not quantified. Second, the strain rate normalization that we applied to all studies is based on testing of cancellous bone in compression and might not be valid for cortical specimens or specimens tested in tension. For instance, Hansen et al. (2008) found the ultimate compressive strength of cortical bone not to increase monotonically with strain rate. Moreover, they found ultimate tensile strength of cortical bone to be negatively correlated with strain rate. Third, except for the study of Charlebois et al. (2010), the ultimate strength-density-morphology relationships that we investigated the present review, are based on the assumption that the bone specimens are loaded along one of the principal eigenvectors of the trabecular architecture. This means that any off axis components of the fabric tensor is ignored when the relationships are derived. In spite of that, the relationships for the pooled data published in the studies of Goulet et al. (1994) and Charlebois et al. (2010) manage to explain 91% and 79% of the variance of the measured compressive ultimate strength reported in these studies, respectively. Fourth, in the studies of Perilli et al. (2007), Perilli et al. (2008), and Tassani et al. (2010) the authors found compressive ultimate strength to be highly correlated with minimum specimen *BVF* and more so than with whole specimen *BVF*. To allow for a meaningful comparison with other studies in the literature, we did not include the relationships based on regression with minimum *BVF*. However, we believe that correlating ultimate strength with minimum *BVF* is meaningful since at least intuitively, the specimens are likely to fail first in the region were the *BVF* and trabecular alignment is least favourable. This is worth considering in future studies that measure ultimate strength of bone cores. However, how small the volume of interest should be for determining the min *BVF* and corresponding fabric tensor is unclear.

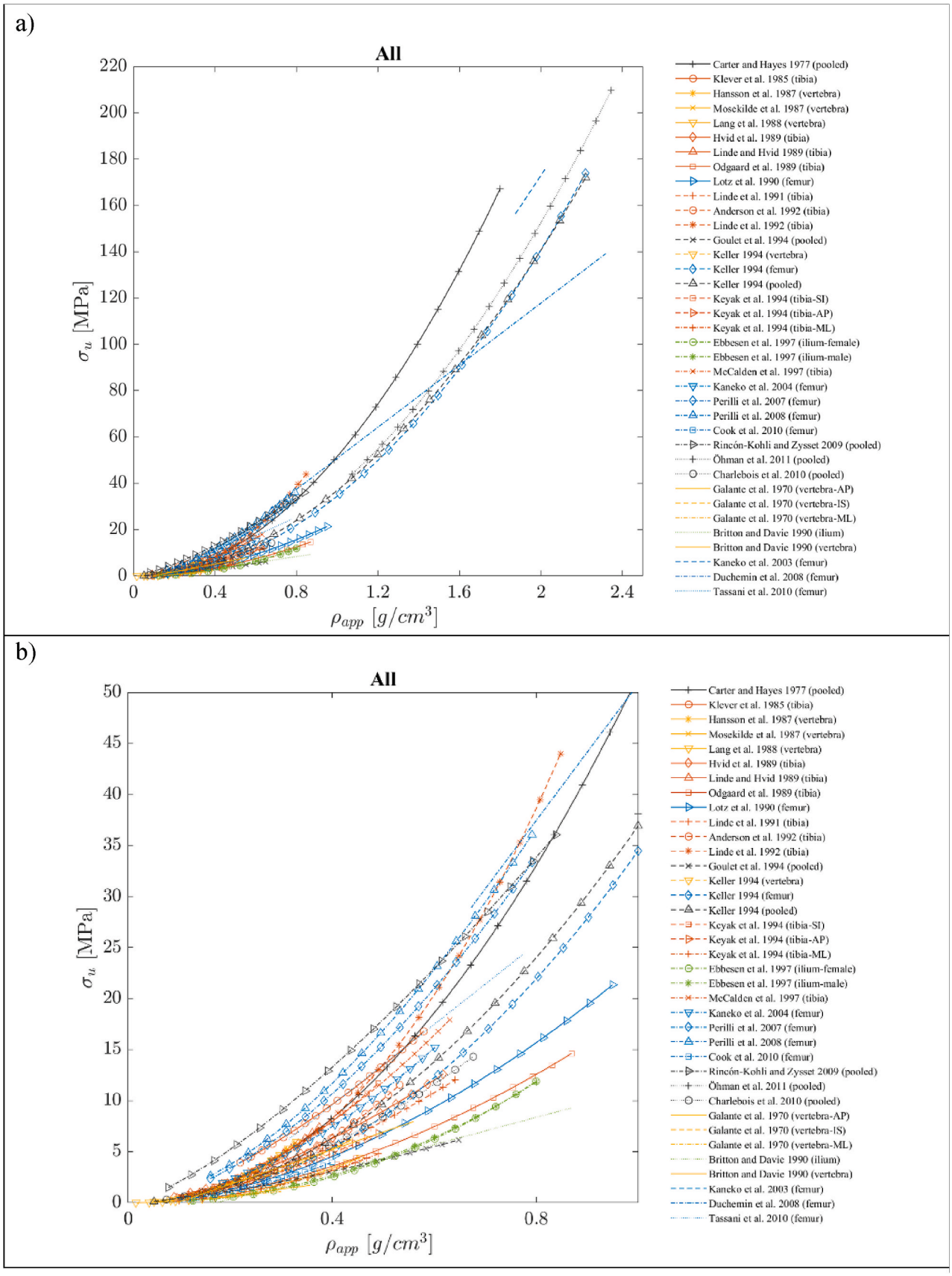

Fig. 1. Compressive ultimate strength-density and compressive ultimate strength-density-morphology relationships reported in the literature normalized to a strain rate of 0.01/s. Full density range (a). Cancellous bone density range (b). Studies are color coded according to anatomic site: Femur (blue), tibia (orange), vertebra (yellow), iliac crest (green), and pooled (black). (For interpretation of the references to color in this figure legend, the reader is referred to the Web version of this article.)

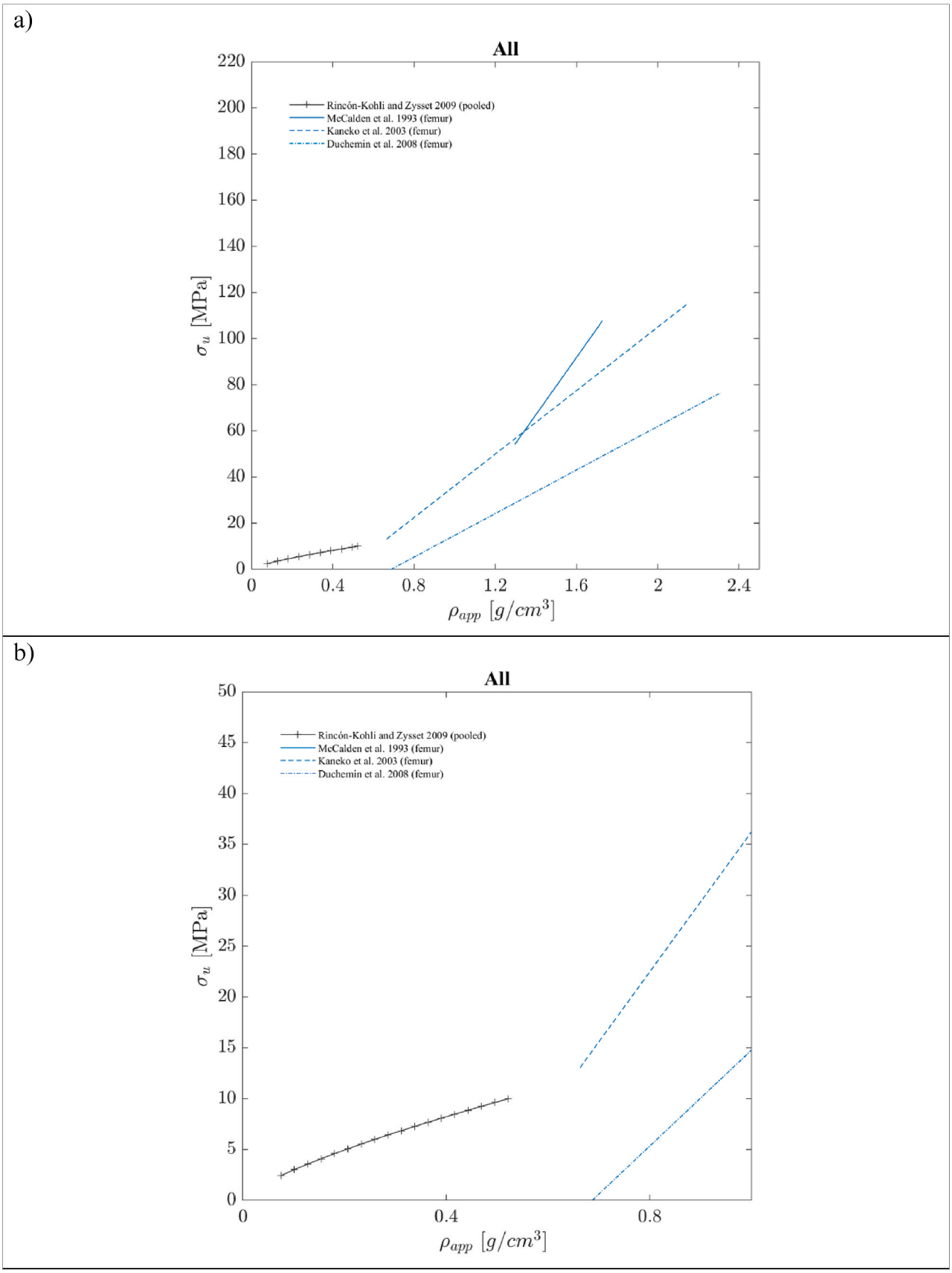

Fig. 2. Tensile ultimate strength-density and tensile ultimate strength-density-morphology relationships reported in the literature normalized to a strain rate of 0.01/s. Full density range (a). Cancellous bone density range (b). Studies are color coded according to anatomic site: Femur (blue) and pooled (black). (For interpretation of the references to color in this figure legend, the reader is referred to the Web version of this article.)

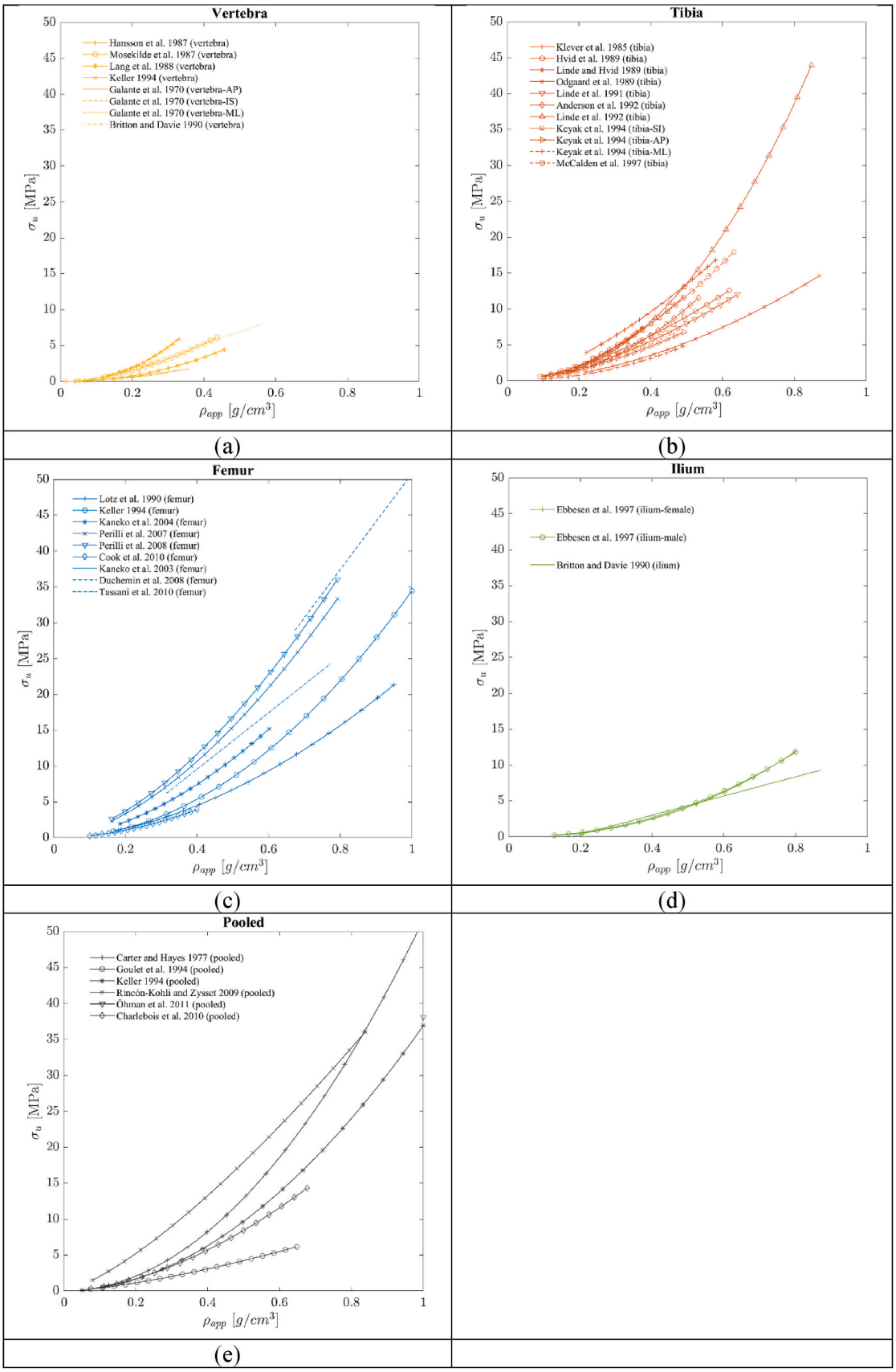

Fig. 3. Compressive ultimate strength-density and compressive ultimate strength-density-morphology relationships in the cancellous bone range for different anatomical sites. (a) vertebra, (b) tibia, (c) femur, (d) ilium and (e) pooled. The results are normalized to a strain rate of 0.01/s.

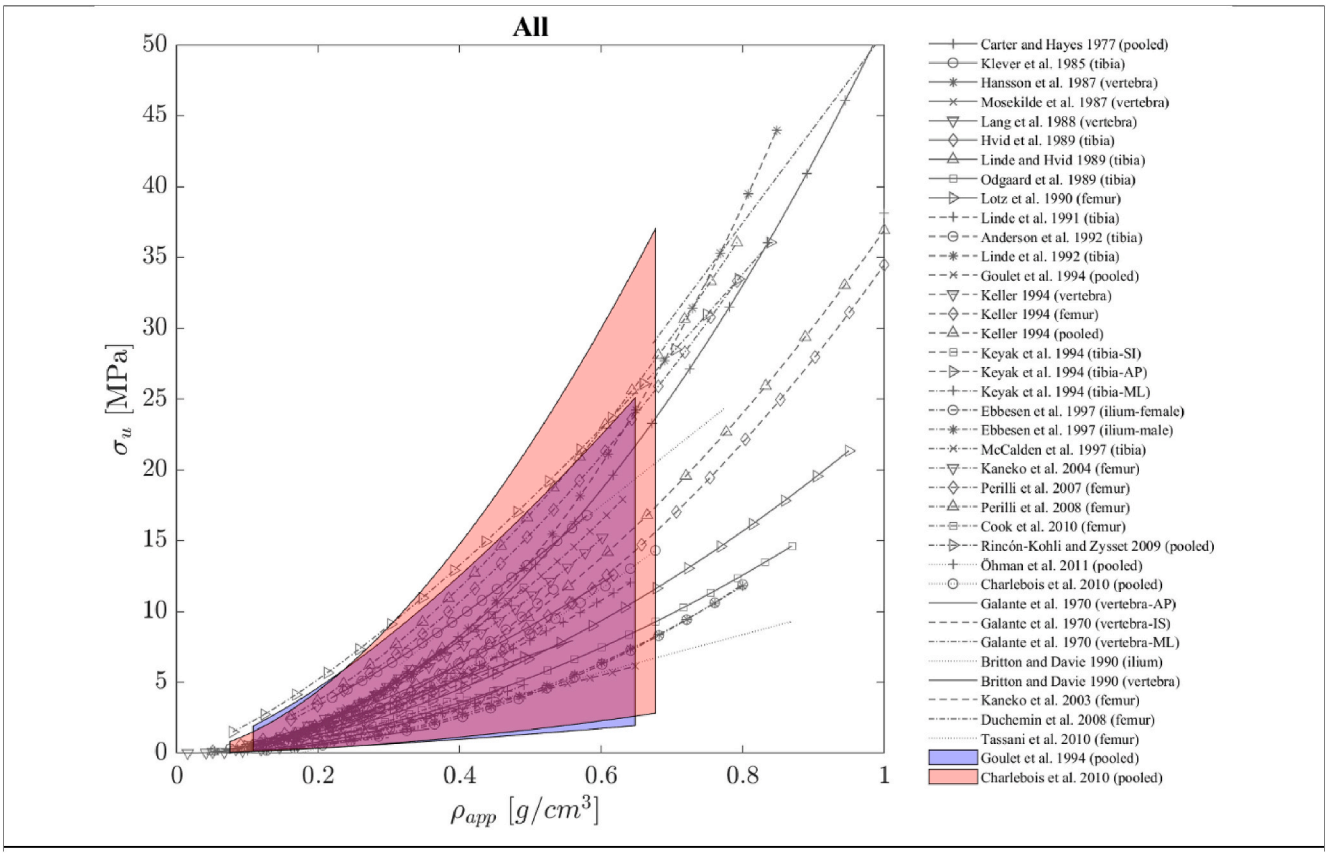

Fig. 4. Compressive ultimate strength-density and compressive ultimate strength-density-morphology relationships reported in the literature in the cancellous bone range, normalized to a strain rate of 0.01/s. The full range of the ultimate strength-density-morphology relationships reported by Goulet et al. (1994) and Charlebois et al. (2010) are overlaid (see Table 4 for details).

4.1. Recommendations

The question that remains is how to best utilize the findings in this review, especially given that information on bone morphology is generally not available from clinical X-ray CT scans due to insufficient image resolution. In other words, mapping morphology based mechanical properties to FEMs based on clinical CT data only, is currently not feasible. However, we believe that advancement of e.g. bone atlases including bone architecture and statistical shape models could help overcome this limitation (Panyasantisuk et al., 2018). This would pave the road towards using non site-specific empirical relationships in our field for mapping mechanical properties to FEMs if future studies support our findings. In this spirit, we would like to make the following recommendations for future studies to consider.

- Although we have found evidence to support that compressive ultimate strength-density-morphology relationships, derived using a wide spectrum of morphology data can explain the inter-study variance in compressive ultimate strength-density relationships in the literature, we believe that our finding should be verified with further testing. This can be done by authors systematically reporting per specimen morphological data in future studies. This would allow for independent validation of our findings apart from allowing for a potential update of the ultimate strength-density-morphology relationships investigated in the present review, once a broader spectrum of test data has been published in the field.
- Our findings indicate a clear need for studies that report the outcome of testing cancellous bone in tension across the full spectrum of bone density and bone morphology. Preferably, such studies would test specimens in both tension and compression with the same specimen preparation procedures to the extent possible. This will allow for stronger conclusions to be drawn on tension-compression asymmetry in ultimate strength than was possible based on this review.
- We did not find ultimate strength-density relationship for cortical bone tested in directions other than along the long axis of long bones. Investigating this aspect of strength-density relationships for cortical bone, tested both in tension and compression, is of considerable interest with respect to improving our understanding of anisotropy of bone tissue.
- Since experimental tests suffer from a large number of artefacts, computational approaches such as FE homogenisation could be engaged to quantify ultimate strength in tension, compression and multiaxial loading on a large collection of human bone samples from various anatomical sites, across the full spectrum of apparent density and architecture. This could potentially lead to a compact set of ultimate strength-density-morphology relationships that can be used for describing ultimate bone strength for different loading directions independent on anatomical site.

5. Conclusion

In summary, we found that differences in bone morphology can explain the inter-study differences in the literature that reports compressive ultimate strength-density relationships in the cancellous bone range. However, we recommend that this finding be further investigated in future studies with richer data. We found insufficient body of literature reporting tensile ultimate-strength relationships for both cancellous and cortical bone. We recommend that further studies be carried out that focus on the measurements of tensile properties of bone on the apparent level.

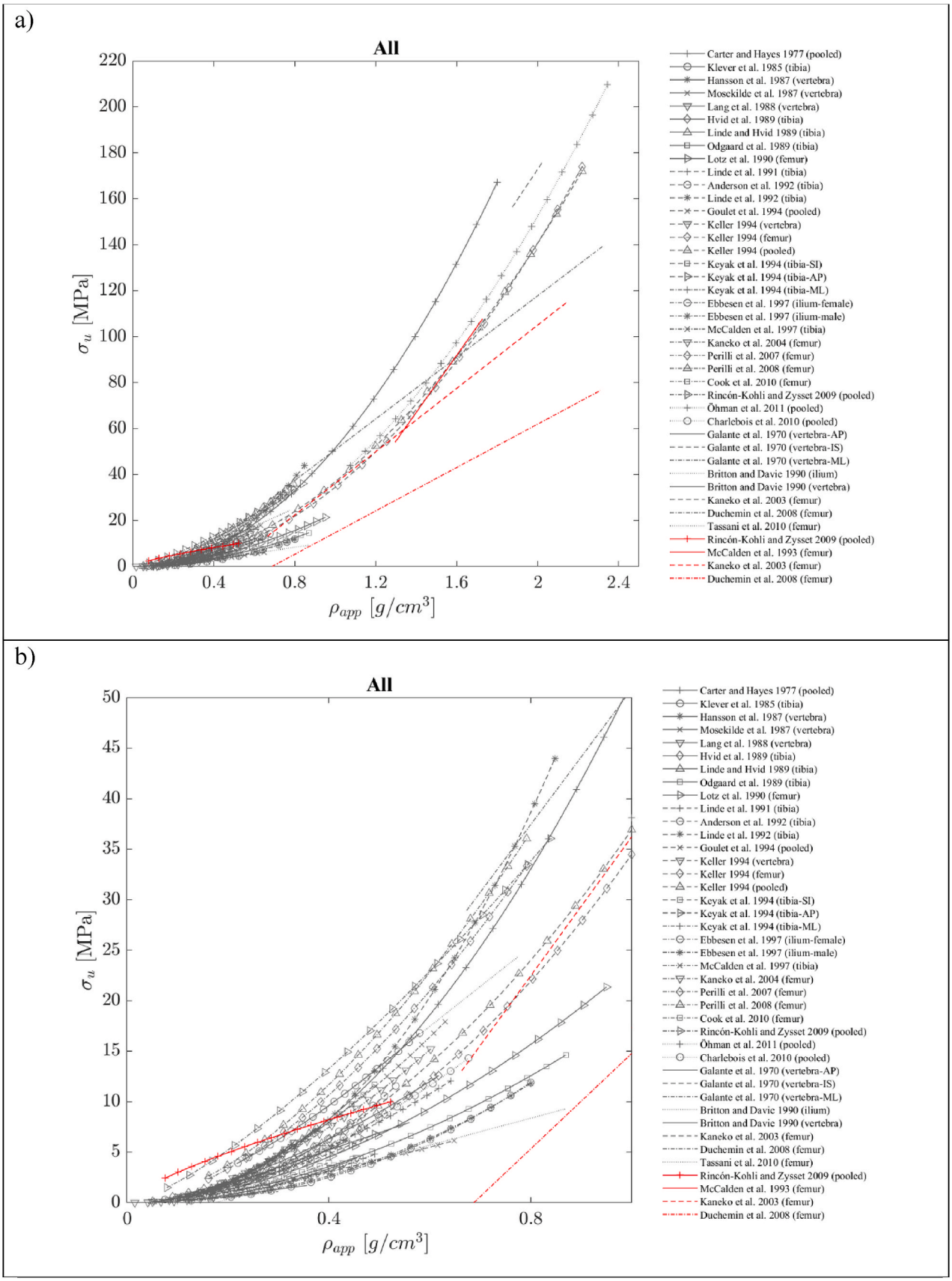

Fig. 5. Compressive and tensile ultimate strength-density and ultimate strength-density-morphology relationships reported in the literature, normalized to a strain rate of 0.01/s. Full density range (a). Cancellous bone density range (b). Compressive ultimate strength-density relationships in grey and tensile ultimate strength-density relationships in red. (For interpretation of the references to color in this figure legend, the reader is referred to the Web version of this article.)

Declaration of competing interest

The authors declare that they have no known competing financial interests or personal relationships that could have appeared to influence the work reported in this paper.

Acknowledgement

This study was supported by the grant #2018-430 of the Strategic Focal Area "Personized Health and Related Technologies" of the ETH Domain, ETH Zurich, Switzerland and the St. Josef 's Hospital Fund, Reykjavik, Iceland.

References

Anderson M J, K.J.H., Skinner, H.B., 1992. Compressive mechanical properties of human cancellous bone after gamma irradiation. J. Bone Joint Surg. 74 (5), 747–752.
Britton, J., Davie, M., 1990. Mechanical properties of bone from iliac crest and relationship to L5 vertebral bone. Bone 11 (1), 21–28.
Burstein, A.H., Reilly, D.T., Martens, M., 1976. Aging of bone tissue: mechanical properties. J. Bone Jt. Surg. Am. Vol. 58 (1), 82–86.
Carter, D.R., Hayes, W.C., 1977. Compressive behavior of bone as a 2-phase porous structure. J. Bone Jt. Surg. Am. Vol. 59 (7), 954–962.
Carter, D.R., Schwab, G.H., Spengler, D.M., 1980. Tensile fracture of cancellous bone. Acta Orthop. Scand. 51 (1–6), 733–741.
Charlebois, M., Pretterklieber, M., Zysset, P.K., 2010. The role of fabric in the large strain compressive behavior of human trabecular bone. J. Biomech. Eng.-Trans. ASME 132 (12).
Cook, R.B., Curwen, C., Tasker, T., Zioupos, P., 2010. Fracture toughness and compressive properties of cancellous bone at the head of the femur and relationships to non-invasive skeletal assessment measurements. Med. Eng. Phys. 32 (9), 991–997.
Cowin, S.C., 1985. The relationship between the elasticity tensor and the fabric tensor. Mech. Mater. 4 (2), 137–147.
Currey, J.D., 2004. Tensile yield in compact bone is determined by strain, post-yield behaviour by mineral content. J. Biomech. 37 (4), 549–556.
Dall'Ara, E., Luisier, B., Schmidt, R., Kainberger, F., Zysset, P., Pahr, D., 2013. A nonlinear QCT-based finite element model validation study for the human femur tested in two configurations in vitro. Bone 52 (1), 27–38.
Duchemin, L., Bousson, V., Raossanaly, C., Bergot, C., Laredo, J.D., Skalli, W., Mitton, D., 2008. Prediction of mechanical properties of cortical bone by quantitative computed tomography. Med. Eng. Phys. 30 (3), 321–328.
Ebbesen, E.N., Thomsen, J.S., Mosekilde, L., 1997. Nondestructive determination of iliac crest cancellous bone strength by pQCT. Bone 21 (6), 535–540.
Eberle, S., Gottlinger, M., Augat, P., 2013. An investigation to determine if a single validated density-elasticity relationship can be used for subject specific finite element analyses of human long bones. Med. Eng. Phys. 35 (7), 875–883.
Galante, J., Rostoker, W., Ray, R., 1970. Physical properties of trabecular bone. Calcif. Tissue Res. 5 (1), 236–246.
Gibson, L.J., 1985. The mechanical behaviour of cancellous bone. J. Biomech. 18 (5), 317–328.
Goulet, R.W., Goldstein, S.A., Ciarelli, M.J., Kuhn, J.L., Brown, M.B., Feldkamp, L.A., 1994b. The relationship between the structural and orthogonal compressive properties of trabecular bone. J. Biomech. 27 (4), 375–389.
Gross, T., Pahr, D.H., Peyrin, F., Zysset, P.K., 2012. Mineral heterogeneity has a minor influence on the apparent elastic properties of human cancellous bone: a SRμCT-based finite element study. Comput. Methods Biomech. Biomed. Eng. 15 (11), 1137–1144.
Gross, T., Pahr, D.H., Zysset, P.K., 2013. Morphology–elasticity relationships using decreasing fabric information of human trabecular bone from three major anatomical locations. Biomech. Model. Mechanobiol. 12 (4), 793–800.
Hansen, U., Zioupos, P., Simpson, R., Currey, J.D., Hynd, D., 2008. The effect of strain rate on the mechanical properties of human cortical bone. J. Biomech. Eng.-Trans. ASME 130 (1).
Hansson, T.H., Keller, T.S., Panjabi, M.M., 1987. A study of the compressive properties of lumbar vertebral trabeculae: effects of tissue characteristics. Spine 12 (1), 56–62.
Harrigan, T., Mann, R., 1984. Characterization of microstructural anisotropy in orthotropic materials using a second rank tensor. J. Mater. Sci. 19 (3), 761–767.
Helgason, B., Perilli, E., Schileo, E., Taddei, F., Brynjolfsson, S., Viceconti, M., 2008. Mathematical relationships between bone density and mechanical properties: a literature review. Clin. Biomech. (Bristol, Avon) 23 (2), 135–146.
Helgason, B., Gilchrist, S., Ariza, O., Vogt, P., Enns-Bray, W., Widmer, R.P., Fitze, T., Palsson, H., Pauchard, Y., Guy, P., Ferguson, S.J., Cripton, P.A., 2016. The influence of the modulus-density relationship and the material mapping method on the simulated mechanical response of the proximal femur in side-ways fall loading configuration. Med. Eng. Phys. 38 (7), 679–689.
Hvid, I., Bentzen, S.M., Linde, F., Mosekilde, L., Pongsoipetch, B., 1989. X-ray quantitative computed tomography: the relations to physical properties of proximal tibial trabecular bone specimens. J. Biomech. 22 (8–9), 837–844.
Kabel, J., Van Rietbergen, B., Odgaard, A., Huiskes, R., 1999. Constitutive relationships of fabric, density, and elastic properties in cancellous bone architecture. Bone 25 (4), 481–486.
Kaneko, T.S., Pejcic, M.R., Tehranzadeh, J., Keyak, J.H., 2003. Relationships between material properties and CT scan data of cortical bone with and without metastatic lesions. Med. Eng. Phys. 25 (6), 445–454.
Kaneko, T.S., Bell, J.S., Pejcic, M.R., Tehranzadeh, J., Keyak, J.H., 2004. Mechanical properties, density and quantitative CT scan data of trabecular bone with and without metastases. J. Biomech. 37 (4), 523–530.
Keaveny, T.M., Wachtel, E.F., Ford, C.M., Hayes, W.C., 1994. Differences between the tensile and compressive strengths of bovine tibial trabecular bone depend on modulus. J. Biomech. 27 (9), 1137–1146.
Keller, T.S., 1994. Predicting the compressive mechanical behavior of bone. J. Biomech. 27 (9), 1159–1168.
Keller, T., Mao, Z., Spengler, D., 1990. Young's modulus, bending strength, and tissue physical properties of human compact bone. J. Orthop. Res. 8 (4), 592–603.
Keyak, J.H., Lee, I.Y., Skinner, H.B., 1994. Correlations between orthogonal mechanical properties and density of trabecular bone: use of different densitometric measures. J. Biomed. Mater. Res. 28 (11), 1329–1336.
Klever, F., Klumpert, R., Horenberg, J., Grootenboer, H., Van Campen, D., Pauly, T., 1985. Global mechanical properties of trabecular bone: experimental determination and prediction from a structural model, Biomechanics: Current Interdisciplinary Research. Springer, pp. 167–172.
Lang, S., Moyle, D., Berg, E., Detorie, N., Gilpin, A., Pappas Jr., N., Reynolds, J., Tkacik, M., Waldron 2nd, R., 1988. Correlation of mechanical properties of vertebral trabecular bone with equivalent mineral density as measured by computed tomography. JBJS 70 (10), 1531–1538.
Linde, F., Hvid, I., 1989. The effect of constraint on the mechanical behaviour of trabecular bone specimens. J. Biomech. 22 (5), 485–490.
Linde, F., Nørgaard, P., Hvid, I., Odgaard, A., Søballe, K., 1991. Mechanical properties of trabecular bone. Dependency on strain rate. J. Biomech. 24 (9), 803–809.
Linde, F., Hvid, I., Madsen, F., 1992. The effect of specimen geometry on the mechanical-behavior of trabecular bone specimens. J. Biomech. 25 (4), 359–368.
Lotz, J.C., Gerhart, T.N., Hayes, W.C., 1990. Mechanical properties of trabecular bone from the proximal femur: a quantitative CT study. J. Comput. Assist. Tomogr. 14 (1), 107–114.
Lotz, J.C., Gerhart, T.N., Hayes, W.C., 1991. Mechanical properties of metaphyseal bone in the proximal femur. J. Biomech. 24 (5), 317–329.
Maquer, G., Musy, S.N., Wandel, J., Gross, T., Zysset, P.K., 2015. Bone volume fraction and fabric anisotropy are better determinants of trabecular bone stiffness than other morphological variables. J. Bone Miner. Res. 30 (6), 1000–1008.
Martin, R.B., Sharkey, N, 2001. Mechanical Effects of Postmortem Changes, Preservation, and Allograft Bone Treatments, Bone Mechanics Handbook, second ed. CRC Press. pp. 20-21-20-24.
Matsuura, M., Eckstein, F., Lochmüller, E.-M., Zysset, P.K., 2008. The role of fabric in the quasi-static compressive mechanical properties of human trabecular bone from various anatomical locations. Biomech. Model. Mechanobiol. 7 (1), 27–42.
McCalden, R.W., McGeough, J.A., 1997. Age-related changes in the compressive strength of cancellous bone. The relative importance of changes in density and trabecular architecture. JBJS 79 (3), 421–427.
McCalden, R.W., McGeough, J.A., Barker, M.B., 1993. Age-related changes in the tensile properties of cortical bone. The relative importance of changes in porosity, mineralization, and microstructure. JBJS 75 (8), 1193–1205.
Morgan, E.F., Keaveny, T.M., 2001. Dependence of yield strain of human trabecular bone on anatomic site. J. Biomech. 34 (5), 569–577.
Morgan, E.F., Bayraktar, H.H., Keaveny, T.M., 2003. Trabecular bone modulus–density relationships depend on anatomic site. J. Biomech. 36 (7), 897–904.
Mosekilde, L., Mosekilde, L., Danielsen, C., 1987. Biomechanical competence of vertebral trabecular bone in relation to ash density and age in normal individuals. Bone 8 (2), 79–85.
Musy, S.N., Maquer, G., Panyasantisuk, J., Wandel, J., Zysset, P.K., 2017. Not only stiffness, but also yield strength of the trabecular structure determined by non-linear μFE is best predicted by bone volume fraction and fabric tensor. J. Mech. Behav. Biomed. Mater. 65, 808–813.
Nishiyama, K.K., Gilchrist, S., Guy, P., Cripton, P., Boyd, S.K., 2013. Proximal femur bone strength estimated by a computationally fast finite element analysis in a sideways fall configuration. J. Biomech. 46 (7), 1231–1236.
Odgaard, A., Hvid, I., Linde, F., 1989. Compressive axial strain distributions in cancellous bone specimens. J. Biomech. 22 (8–9), 829–835.
Öhman, C., Baleani, M., Pani, C., Taddei, F., Alberghini, M., Viceconti, M., Manfrini, M., 2011. Compressive behaviour of child and adult cortical bone. Bone 49 (4), 769–776.
Pahr, D.H., Zysset, P.K., 2009. From high-resolution CT data to finite element models: development of an integrated modular framework. Comput. Methods Biomech. Biomed. Eng. 12 (1), 45–57.
Panyasantisuk, J., Dall'Ara, E., Pretterklieber, M., Pahr, D.H., Zysset, P.K., 2018. Mapping anisotropy improves QCT-based finite element estimation of hip strength in pooled stance and side-fall load configurations. Med. Eng. Phys. 59, 36–42.
Perilli, E., Baleani, M., Öhman, C., Baruffaldi, F., Viceconti, M., 2007. Structural parameters and mechanical strength of cancellous bone in the femoral head in osteoarthritis do not depend on age. Bone 41 (5), 760–768.
Perilli, E., Baleani, M., Öhman, C., Fognani, R., Baruffaldi, F., Viceconti, M., 2008. Dependence of mechanical compressive strength on local variations in microarchitecture in cancellous bone of proximal human femur. J. Biomech. 41 (2), 438–446.
Pisu, M., Kopperdahl, D.L., Lewis, C.E., Saag, K.G., Keaveny, T.M., 2019. Cost-effectiveness of osteoporosis screening using biomechanical computed tomography for patients with a previous abdominal CT. J. Bone Miner. Res. 34 (7), 1229–1239.

Poelert, S., Valstar, E., Weinans, H., Zadpoor, A.A., 2013. Patient-specific finite element modeling of bones. Proc. Inst. Mech. Eng. H 227 (4), 464–478.
Reilly, D.T., Burstein, A.H., 1975. The elastic and ultimate properties of compact bone tissue. J. Biomech. 8 (6), 393–405.
Rice, J., Cowin, S., Bowman, J., 1988. On the dependence of the elasticity and strength of cancellous bone on apparent density. J. Biomech. 21 (2), 155–168.
Rincón-Kohli, L., Zysset, P.K., 2009. Multi-axial mechanical properties of human trabecular bone. Biomech. Model. Mechanobiol. 8 (3), 195–208.
Røhl, L., Larsen, E., Linde, F., Odgaard, A., Jørgensen, J., 1991. Tensile and compressive properties of cancellous bone. J. Biomech. 24 (12), 1143–1149.
Schileo, E., Dall'ara, E., Taddei, F., Malandrino, A., Schotkamp, T., Baleani, M., Viceconti, M., 2008. An accurate estimation of bone density improves the accuracy of subject-specific finite element models. J. Biomech. 41 (11), 2483–2491.
Snyder, S.M., Schneider, E., 1991. Estimation of mechanical properties of cortical bone by computed tomography. J. Orthop. Res. 9 (3), 422–431.
Sternheim, A., Giladi, O., Gortzak, Y., Drexler, M., Salai, M., Trabelsi, N., Milgrom, C., Yosibash, Z., 2018. Pathological fracture risk assessment in patients with femoral metastases using CT-based finite element methods. A retrospective clinical study. Bone 110, 215–220.
Sun, S.-S., Ma, H.-L., Liu, C.-L., Huang, C.-H., Cheng, C.-K., Wei, H.-W., 2008. Difference in femoral head and neck material properties between osteoarthritis and osteoporosis. Clin. BioMech. 23, S39–S47.
Tanaka, Y., Kokubun, S., Sato, T., Iwamoto, M., Sato, I., 2001. Trabecular domain factor and its influence on the strength of cancellous bone of the vertebral body. Calcif. Tissue Int. 69 (5).
Tassani, S., Öhman, C., Baleani, M., Baruffaldi, F., Viceconti, M., 2010. Anisotropy and inhomogeneity of the trabecular structure can describe the mechanical strength of osteoarthritic cancellous bone. J. Biomech. 43 (6), 1160–1166.
Turner, C.H., Cowin, S.C., Rho, J.Y., Ashman, R.B., Rice, J.C., 1990. The fabric dependence of the orthotropic elastic constants of cancellous bone. J. Biomech. 23 (6), 549–561.
Viceconti, M., Davinelli, M., Taddei, F., Cappello, A., 2004. Automatic generation of accurate subject-specific bone finite element models to be used in clinical studies. J. Biomech. 37 (10), 1597–1605.
Wang, X., Shen, X., Li, X., Agrawal, C.M., 2002. Age-related changes in the collagen network and toughness of bone. Bone 31 (1), 1–7.
Zysset, P.K., 2003. A review of morphology–elasticity relationships in human trabecular bone: theories and experiments. J. Biomech. 36 (10), 1469–1485.
Zysset, P.K., Goulet, R.W., Hollister, S.J., 1998. A global relationship between trabecular bone morphology and homogenized elastic properties. J. Biomech. Eng. 120 (5), 640–646.